

# Quantitative geophysical pore-type characterization and its geological implication in carbonate reservoirs

Luanxiao Zhao<sup>1\*</sup>, Mosab Nasser<sup>1,2</sup> and De-hua Han<sup>1</sup>

<sup>1</sup>University of Houston, <sup>2</sup>Maersk Oil America Inc.

Received June 2012, revision accepted January 2013

## ABSTRACT

This paper discusses and addresses two questions in carbonate reservoir characterization: how to characterize pore-type distribution quantitatively from well observations and seismic data based on geologic understanding of the reservoir and what geological implications stand behind the pore-type distribution in carbonate reservoirs. To answer these questions, three geophysical pore types (reference pores, stiff pores and cracks) are defined to represent the average elastic effective properties of complex pore structures. The variability of elastic properties in carbonates can be quantified using a rock physics scheme associated with different volume fractions of geophysical pore types. We also explore the likely geological processes in carbonates based on the proposed rock physics template. The pore-type inversion result from well log data fits well with the pore geometry revealed by a FMI log and core information. Furthermore, the S-wave prediction based on the pore-type inversion result also shows better agreement than the Greensberg-Castagna relationship, suggesting the potential of this rock physics scheme to characterize the porosity heterogeneity in carbonate reservoirs. We also apply an inversion technique to quantitatively map the geophysical pore-type distribution from a 2D seismic data set in a carbonate reservoir offshore Brazil. The spatial distributions of the geophysical pore type contain clues about the geological history that overprinted these rocks. Therefore, we analyse how the likely geological processes redistribute pore space of the reservoir rock from the initial depositional porosity and in turn how they impact the reservoir quality.

**Key words:** Carbonates, Pore type, Dolomitization.

## INTRODUCTION

Carbonate rocks are considered a major host rock for hydrocarbon reservoirs, making up almost 60% of the world's proven reserves. They significantly differ from siliciclastic reservoirs because of their different depositional environments and complicated diagenetic processes (Anselmetti and Eberli 1993; Lucia 1995, 1999). Due to the high chemical reactivity of carbonate material, these rocks constantly undergo intense cementation, dissolution and dolomitization, which are

strongly influenced by factors such as water depth, temperature and pressure (Brie, Johnson and Nurmi 1985). Such intense diagenetic history can alter the mineralogy and texture of the original framework, thereby causing carbonate rocks to exhibit wide variations in pore types, such as interparticle, intercrystal, moldic, vuggy, intraframe and microcracks.

One of the main challenges of quantitative reservoir characterization in carbonates lies in identifying producible, economic reserves and distinguishing them from low recoverable reserves. Insights into producibility can be gained from permeability prediction, which is strongly related to the complex pore structures mentioned earlier (Anselmetti and Eberli 1993; Lucia 1995, 1999; Baechle, Weger and Eberli 2005;

---

\*E-mail: zhaoluanxiao@gmail.com

Sun *et al.* 2006; Baechle *et al.* 2007). As a consequence, predicting pore-type distribution from well log and seismic data is essential for delineating a reservoir's architecture and flow properties. Such a task is often achieved by employing various rock physics transforms that link rock properties to geophysical observations. In this paper, we will present how to perform rock physics inversion to quantitatively estimate pore-type distribution from geophysical measurements.

Previous laboratory studies on carbonate rocks have showed that measured velocity-porosity data have a wide range of scatter (Rafavich, Kendall and Todd 1984; Wang, Hirsche and Sedgwick 1991; Anselmetti and Eberli 1997; Assefa, McCann and Sothcott 2003; Eberli *et al.* 2003; Baechle *et al.* 2005). Carbonate rocks are well cemented and grain contact elasticity is not considered as an important parameter affecting carbonate's elastic properties (Brie *et al.* 1985; Han 2004). Hence, for a given mineral composition and fluid type, such scattering on velocity-porosity cross-plots could be mainly related to the pore-type effects (Wang *et al.* 1991; Anselmetti and Eberli 1991; Eberli *et al.* 2003; Sayers 2008). In general, it is found that frame-embedded pores, such as moldic and vuggy pores, are round and very resistant to pressure change. Conversely, thin penny-shaped cracks tend to be flat and will have much lower stiffness, thus being easily affected by seismic wave propagation.

Different documented rock physics studies have incorporated the pore-type effect into predicting and modelling carbonate's elastic properties. Pores in carbonates are often modelled as idealized ellipsoidal inclusions characterized by their aspect ratio (minor axis divided by major axis). By using a long-wavelength first-order scattering theory, Kuster and Toksöz (1974) derived an expression for the effective moduli of a composite media of inclusions with different pore geometries in a background host material. The major constraint in this theory is that the ratio of porosity and aspect ratio should be less than or equal to 1. This means that for ellipsoidal cracks (aspect ratio is about 0.01), this theory can calculate effective media properties only up to a porosity of 1%. This limitation restricts the use of this model. To overcome the dilute concentration, Kumar and Han (2005) employed a differential effective medium (DEM) scheme (Berryman 1992; Mavko, Mukerji and Dvorkin 2009) by inserting dry inclusions to obtain the rock's effective properties. Fluid substitution to the desired saturation is then performed using Gassmann's equation. They quantified the pore-type effect by dividing the total pore space into stiff vuggy pores characterized by high-aspect ratios, interparticle pores with intermediate aspect ratios and compliant micropores with lower aspect ratios. Based on Ku-

mar's work, Xu and Payne (2009) developed an extended Xu-White model by introducing clay-related pores into a carbonate's pore system. Wet clay-related pores behave as if they are isolated and hence result in a high-frequency seismic response. Agersborg *et al.* (2008) implemented a T-matrix approach (Jakobsen, Hudson and Johansen 2003a; Jakobsen, Johansen and McCann 2003b) to describe velocity scattering and dispersion thanks to the complex pore structures in carbonates. Due to the overall complexity of the interrelationships among carbonate properties, we are still far from fully understanding how the pore type coupled with other physical properties such as fluid flow, pore pressure, mineralogy and fluid-solid reactivity affect the velocity of carbonates (Vanorio, Scotellaro and Mavko 2008). What we are attempting here is to identify the possible contribution of variations in pore types to the elastic moduli of carbonates. In this paper, our pore-type characterization scheme will draw heavily on previous work by both Kumar and Han (2005) and Xu and Payne (2009).

As we mentioned, geological processes like dissolution, leaching, dolomitization and cementation can enhance and destroy porosity continuously. On the other hand, differential compaction, faulting and solution collapse can introduce cracks and micro-fractures in carbonates. Such origin and modification of porosity are very important for understanding carbonate reservoirs. In other words, pore types have recorded the story that they underwent in the geological history of carbonates. This implies that if we can determine the pore-type distribution in carbonates, then the geological processes, especially diagenesis, can potentially be restored based on the geological understanding of the reservoir. We will demonstrate how to interpret carbonate's geological history from pore-type distribution and discuss the implications to reservoir properties.

The whole approach is evaluated using real core information and well log and seismic data from a Cretaceous (Albian) carbonate heavy oil reservoir, which is located in the Campos Basin, offshore Brazil. Proximally, Albian carbonates are deposited from higher energy shallower-water conditions during the early Albian (112–108 Ma) to lower energy lagoonal or central platform settings by late Albian times (102–100 Ma) (Ogiesoba *et al.* 2011). The reservoir rocks are highly heterogeneous. Figure 1 shows thin sections for several core plugs representative of the Albian carbonate formation. The carbonates show a grain-supported texture with variable porosity ranging from crack-like pores to separate-vuggy pores, which indicate that these rocks are modified and imprinted by complicated diagenetic history.

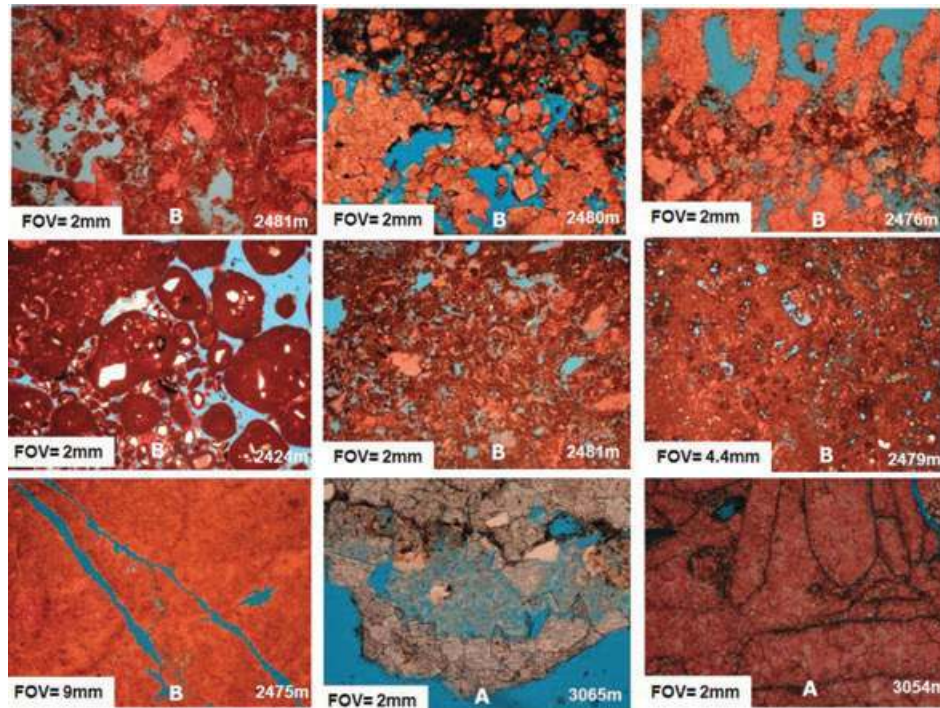


Figure 1 Thin sections for nine core plugs from a carbonate reservoir in the Campos Basin, offshore Brazil. Blue parts represent pore space where A and B indicate that they are from two different wells. The burial depth in metres and field of view are also denoted.

## ROCK PHYSICS OF CARBONATES

### Geophysical pore types in carbonates

Pores in carbonates can be classified based on their size, visibility and diagenetic and geometric complexity (Dunham 1962; Choquette and Pray 1970; Lucia 1999). Despite that all these classifications are useful for characterizing petrophysical properties, relating these descriptions to a geophysical response is very challenging. This is because the seismic wavelength is often much larger than the microstructure's scale size, so the wave can 'see' only the average effective properties of complex pore structures and not the individual pores and cracks (Jakobsen and Chapman 2009). Therefore, we simplify the complex pore network into three geophysical pore types to reasonably represent the acoustic and pressure response of carbonate reservoir rocks (Sain *et al.* 2008; Xu and Payne 2009). The three geophysical pore types are classified as: (1) reference pores that serve as the background trend. They consist largely of interparticle and intercrystal pores and are considered as the dominant pore type in carbonates. (2) Stiff pores with high-aspect ratios, which represent moldic and vuggy pores and are usually formed as a result of dissolved grains and fossil chambers. (3) Cracks with lower aspect ratios, which represent micro-fractures and micro-cracks. They can occur

due to differential compaction, faulting and solution collapse in carbonates (Lucia 1999). The above pore types are termed geophysical pore types in our study.

A detailed description of this classification is shown in Fig. 2. The aspect ratios of these pore types can be locally determined from core measurements and a petrographic

	Pore types		
Petrophysical	Vuggy(Moldic)	Interparticle(Intercystal)	Microcracks
Geophysical	Stiff	Reference	Cracks
Aspect Ratio	0.7-0.8	0.12-0.15	0.01-0.02
Image			
Pore systems			

Figure 2 Geophysical pore-type classification in carbonates. The first two thin sections, which indicate stiff pores and reference pores, are from Lucia (1999). Detailed description of the geophysical pore systems is as follows: red ellipse with a higher aspect ratio represents round stiff pores (vuggy or moldic pores), black ellipse with an intermediate aspect ratio represents reference pores (interparticle porosity) and purple ellipse with a low-aspect ratio indicates crack-like pores.

description of thin sections from different reservoirs. They can also be quantified using pore-geometry spectral analysis obtained from SEM images of thin sections, or from digital image analysis. The three pore types can coexist in pore space but the well log and seismic response are generally controlled by the dominant pore type. In this way, the pore systems of carbonates can be classified as reference pores with stiff pores and reference pores with cracks (Xu and Payne 2009).

### Rock physics modelling in carbonates

Effective medium models have versatile features to capture approximate trends for the effects of porosity, pore shape and mineralogy on elastic properties. The differential effective medium (DEM) theory provides a tool to calculate the effective bulk and shear moduli for different pore types even when the volume concentrations are no longer small (Berryman 1992; Mavko *et al.* 2009). This scheme simulates porosities in a composite of two phases by incrementally adding a small amount of pores (phase 2) into a matrix (phase 1). The coupled system of ordinary differential equations can then be written as:

$$(1 - \phi) \frac{d}{d\phi} [K^*(\phi)] = (K_2 - K^*) P^{(*2)}(\phi), \quad (1)$$

$$(1 - \phi) \frac{d}{d\phi} [\mu^*(\phi)] = (\mu_2 - \mu^*) Q^{(*2)}(\phi), \quad (2)$$

with the initial conditions  $K^*(0) = K_1$  and  $\mu^*(0) = \mu_1$ , where  $K_1$  and  $\mu_1$  are the matrix bulk and shear moduli respectively.  $K_2$  and  $\mu_2$  are the bulk and shear moduli of the inclusion phase respectively.  $\phi$  is the porosity and  $d\phi$  is the incremental change in porosity.  $P^{(*2)}$  and  $Q^{(*2)}$  are the geometrical factors depending on the aspect ratios of the elliptical pores (Wu 1966).

Some of the properties of this scheme listed below are of particular interest, since they are very important in determining their applicability in carbonates.

a) This scheme assumes that the cavities are isolated with respect to fluid flow and in response, it simulates a high-frequency response for a saturated rock. To make this scheme applicable to field low-frequency situations, one should estimate the dry rock response using this scheme and then apply Gassmann's equation to perform fluid substitution (Mavko *et al.* 2009).

b) In carbonates, we consider rocks with vuggy pores and moldic pores, due to dissolution processes, to resemble the physical realization of DEM rather than other effective medium methods (Ruiz 2009). However, the process of incre-

mentally adding inclusions to the matrix is a thought experiment and should not be taken to provide an accurate description of the true evolution of rock porosity in nature (Mavko *et al.* 2009).

c) The DEM scheme does not treat each constituent symmetrically. More precisely, this scheme identifies one of the constituents as a host or matrix material in which inclusions of the other constituent(s) are embedded, so the numerical result is path dependent. That is why DEM is said to be asymmetric. In contrast, for instance, the Self Consistent (SC) scheme does not identify any specific host material but treats the composite as an aggregate of all the constituents. That is why SC is often said to be symmetric. We take care of this asymmetry of DEM by proportionally adding dilute concentrations of different dry pores at each step (Keys and Xu 2002). Actually, experience suggests that this is not a problem. Adding high-aspect ratio spherical pores first shows little difference in comparison with adding small aspect ratio cracks first (Kumar and Han 2005).

In this work, we follow Xu and Payne's (2009) extended Xu-White model for carbonates, in which the total pore space can be divided into four components: (i) clay-related pores, (ii) stiff pores, (iii) reference pores and (iv) cracks. We mix minerals present in the rock using Voigt-Reuss-Hill averages to obtain the elastic moduli of the solid rock matrix. The clay-related pores with bound water are added first and will be included in the solid material for fluid substitution and then three geophysical pore types are added using the DEM scheme to obtain the dry effective bulk and shear moduli. The fluid modulus can be modelled using Wood's suspension model to take into account the fluid saturation effect. Finally, Gassmann's fluid substitution method is performed and the elastic response of the saturated rock is calculated. Detailed rock physics modelling steps are given in Fig. 3.

Figure 4 shows the effect of pore type on a P-wave velocity-porosity cross-plot that always lies within the rigorous Hashin-Shtrikman bounds. Aspect ratios of the stiff pores, reference pores and cracks are assumed to be 0.7, 0.15 and 0.02 respectively. The reference line represents the velocity-porosity relationship with only reference pores, which could help us distinguish trends for rocks with different dominant pore types. Curves below the reference line represent the pore systems with increasing fractions of cracks and those above it suggest increasing fractions of stiff pores. As expected, stiff pores make the velocity show little sensitivity to porosity change, while crack-like pores result in significantly softening the rock. This implies that large vuggy pores may increase the pore space dramatically without increasing the overall elastic



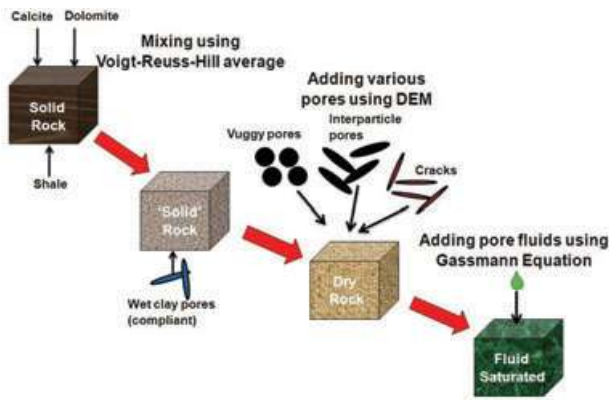


Figure 3 Detailed steps of rock physics modelling in carbonates (After Xu and Payne 2009)

compressibility of the rock. On the contrary, small concentrations of crack-like pores can be effective in reducing velocity. Such an introduced modelling velocity-porosity cross-plot can be regarded as a rock physics template for carbonates. The advantage of this template is that it quantifies the effect of volume fractions of different pore types on the elastic properties of the rock. If a data point lies on the 20% stiff pore line, it indicates that 20% of the total pore space has stiff porosity and the remainder 80% has reference porosity.

We cast data points from well log data, colour-coded by shale content, in a carbonate reservoir offshore Brazil. Core analysis shows that quartz and feldspar constitute 60% of the shale content, while the other 40% of the shale content is composed of clay. Also, given that the heavy oil’s elastic properties are very close to those of brine (Table 1), this rock physics template for saturated brine can also represent the

Table 1. Elastic properties of fluids in reservoir rock from lab measurements

	Bulk Modulus (Gpa)	Shear Modulus (Gpa)	Density (g/cm <sup>3</sup> )
Brine	3.0	0	1.04
Heavy Oil	2.1	0	0.94

elastic response of carbonate rocks saturated with heavy oil. Most of the data fall between the 100% stiff pores line and the 100% cracks line. It is evident that they show large scattering even when the reservoir rocks are very clean. The dominant pore type in the limestone unit appears to be reference pores, while more cracks than expected are in the dolostone unit. Simulated elastic properties of the carbonate’s Vp/Vs ratio versus P-impedance are displayed in Fig. 5. P-impedance always decreases from the mineral point with increasing porosity, however the Vp/Vs ratios are more complicated due to the different pore types. Generally speaking, cracked carbonates tend to have a higher Vp/Vs ratio than those dominated by stiff pores. This suggests that the shear waves are more affected by the presence of cracks than stiff pores. From the cross-plot, we can also conclude that the dolostone unit is more cracked than the calcite unit. This finding can be helpful when applying this template to interpret seismic inversion results.

The geological history of carbonate rocks

When the velocity-porosity template is built, it is of interest to ask what kinds of geological processes control such a

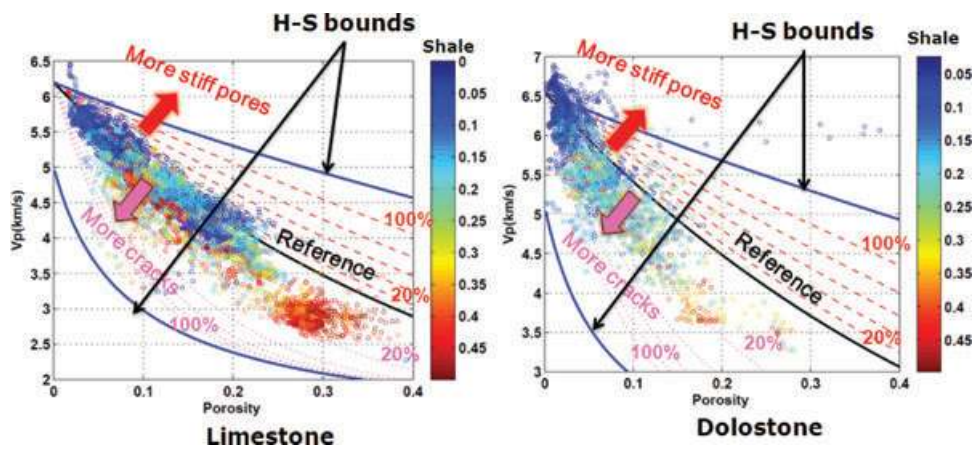


Figure 4 Illustration of pore-type effect on the P-wave velocity-porosity relationship. The figure on the left is a calcite based solid matrix and on the right is a dolomite based solid matrix. The clay content is assumed to be 5% and the fluid phase is brine. All of the data points are from well log data in the carbonate reservoir offshore Brazil.

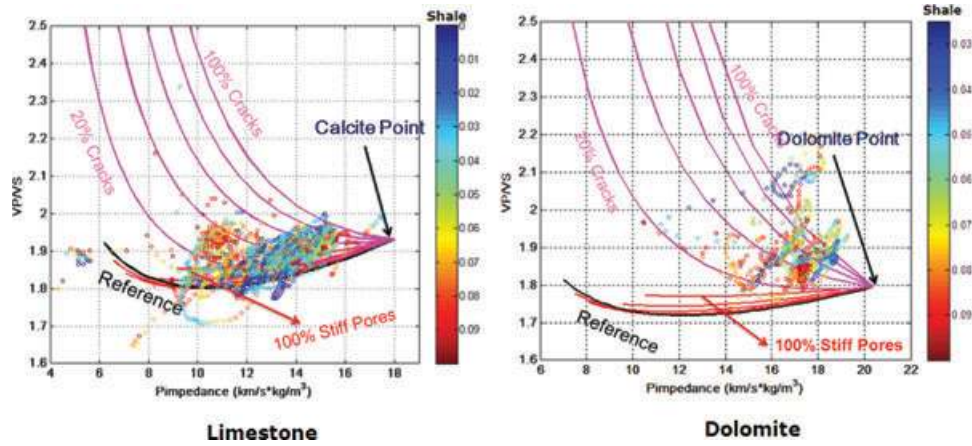


Figure 5 Rock elastic properties simulation from a rock physics model in carbonates displayed as P- and S-wave velocity ratio versus acoustic impedance. The figure on the left is a calcite based solid matrix and on the right is a dolomite based solid matrix. All of the data points are from well log data in the carbonate reservoir offshore Brazil.

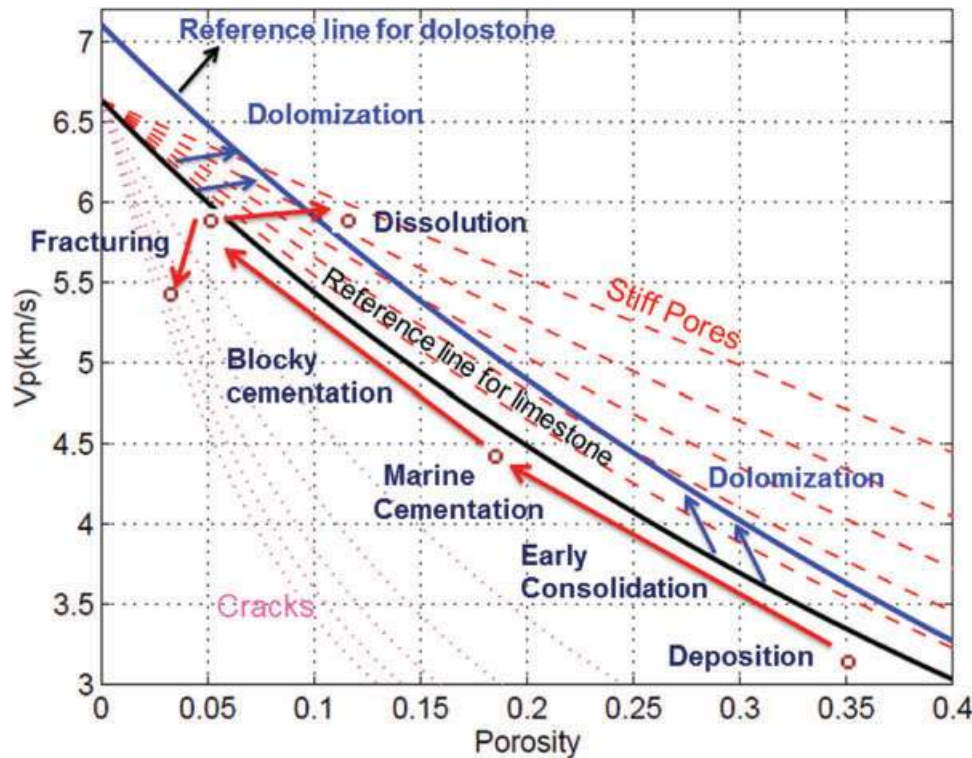


Figure 6 A carbonate’s geological history based on P-wave velocity and porosity relationship. The black and blue lines represent reference lines for limestone and dolostone respectively. The red arrows illustrate different geological processes for a carbonate’s evolution history and the blue arrows from the reference line for limestone to dolostone indicate the dolomitization process.

physical relationship. One possible geological story based on our rock physics modelling result is shown in Fig. 6. It is clear that carbonate rocks are initially controlled by patterns of depositional textures and the porosity types have commonly interparticle porosity. Cementation and compaction occlude

pore space and systematically reduce pore size along the reference line. If no chemical reactions take place, the porosity type stays as interparticle during this mechanical process. Selective dissolution processes typically form separate vugs or moldic porosity by selectively dissolving grains composed of

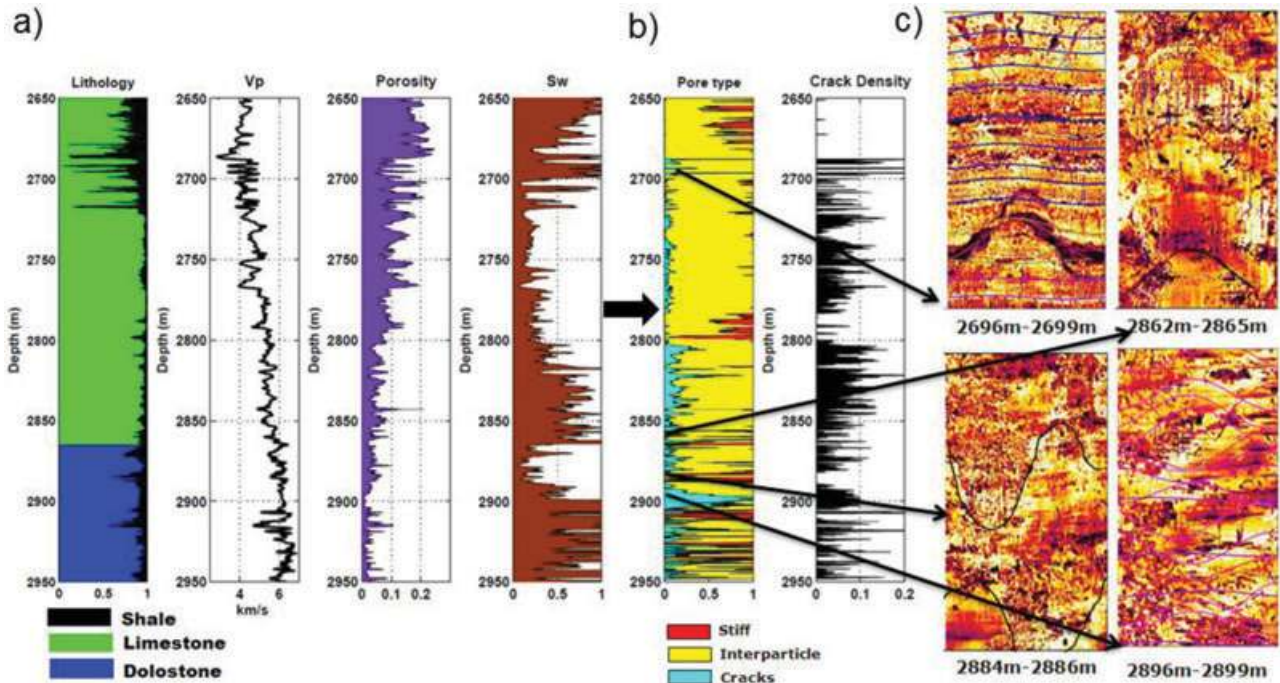


Figure 7 (a) Log data from well A in the carbonate reservoir offshore Brazil. The lithology content, P-wave velocity, bulk porosity and water saturation are displayed as a function of depth. (b) Geophysical pore-type inversion result for well A. Area of red, yellow and blue colours represent volume concentrations of stiff, interparticle and crack-like pores in the pore space, respectively. (c) OMRI-CAST borehole images that are used to verify the pore-type inversion result. The arrows point from the corresponding depth of the inversion result to those observed on the OMRI-CAST image.

unstable minerals that in turn make the rock stiffer. However, the porosity often does not increase much because the calcium and carbonate ions produced by dissolution of unstable aragonite are precipitated as calcite cementation (Lucia 1999). Fracturing is closely related to overburden and differential compaction, massive dissolution and collapse, thus increasing the connection between separate vugs and enhancing permeability dramatically. Sometimes, large-scale fracturing can be associated with karst related processes. The elastic response of fracturing makes rocks considerably more compliant compared with other pore types. Another important geological process associated with dolostone reservoirs is dolomitization, which reorganizes pore space through a microchemical process of calcium dissolution and dolomite precipitation. We simplify such a geological process in our rock physics template as the reference line of limestone moving towards the reference line of dolostone. In the early stage of sedimentation, dolomitization decreases porosity because of a net addition of dolomite. But if dolomitization occurs in a later geological age, it can preserve porosity due to increasing resistance to compaction in contrast to limestone (Lucia 1999).

The geological story we tell here illustrates how we can identify and link different geological processes given the pore-type information. Nonetheless, geological processes in carbonates are very complicated, since they can overlap in diagenetic timing and therefore have an effect on each other.

#### Geophysical pore-type inversion algorithm

Since our rock physics template can quantify the effects of pore type on elastic properties, we can make an estimate of the volume fractions of the different pore types with given bulk porosity and P-wave velocity from well log data or seismic data. The prerequisite for this work is that mineralogy effects and fluid saturations should be locally calibrated. Kumar and Han (2005) developed a pore-type inversion scheme, in which the background velocity is calculated using Wyllie's time-average equation. However, in this case we used our modelling reference line as the background trend. Another point that needs to be mentioned here is that the inversion algorithm is constrained by allowing the coexistence of only two pore types, either reference pores with stiff pores or reference pores with cracks. The main inversion steps are as follows:



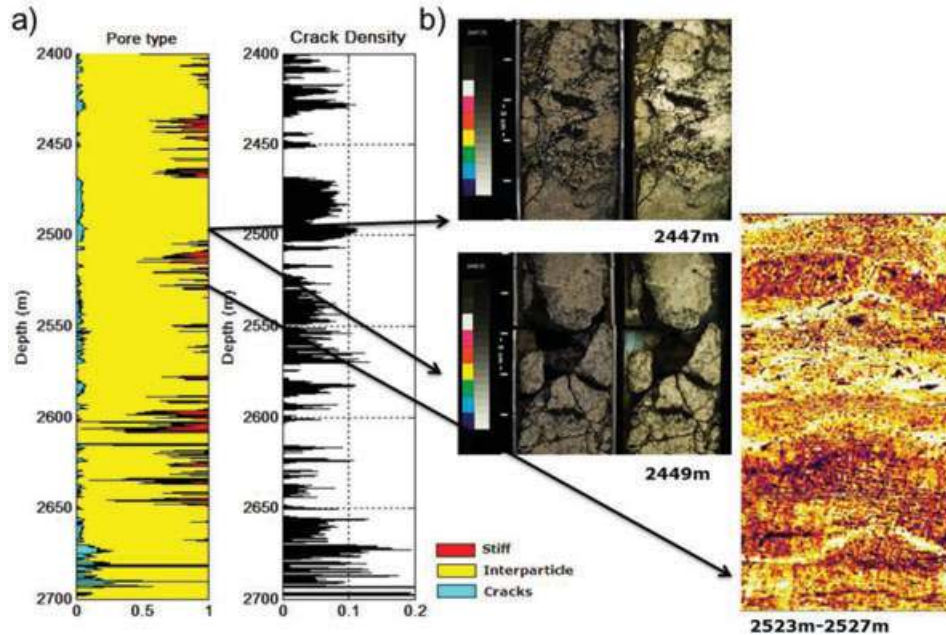


Figure 8 (a) Geophysical pore-type inversion result for well B from the carbonate reservoir offshore Brazil. Area of red, yellow and blue colours represent volume concentrations of stiff, interparticle and crack-like pores in the pore space, respectively. (b) OMRI-CAST image logs and core photos that are used to verify the pore-type inversion result. The arrows point from the corresponding depth of the inversion result to those observed on the OMRI-CAST image.

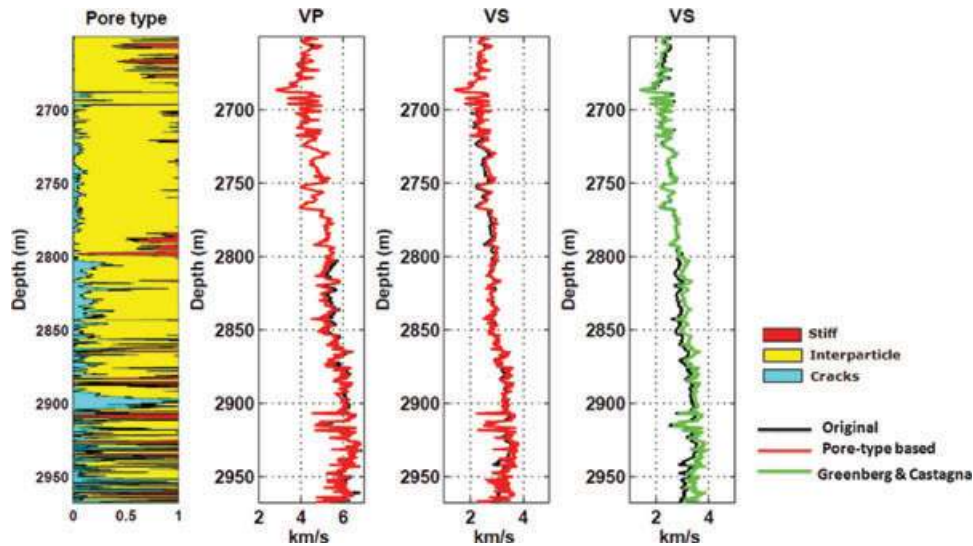


Figure 9 Shear-wave velocity prediction from the pore-type inversion result for well A. The black line indicates original well log data, the red line indicates predicted S-wave velocity based on the pore-type inversion result and the green line indicates predicted S-wave velocity using the Greenberg-Castagna relationship.

1. Define the aspect ratio of the three geophysical pore types in the carbonate reservoir.
2. Input the measured velocity  $V_p$  and porosity  $\phi_0$  from well log data.
3. Assume that only reference pores make the pore spaces and then use the DEM theory and the modelling method to calculate  $V_{p_{reference}}$  given porosity  $\phi_0$  and aspect ratio  $\alpha_{reference}$ .



4. If the measured velocity  $Vp$  is greater than  $Vp_{reference}$ , use  $\alpha_1 = \alpha_{reference}$ ,  $\alpha_2 = \alpha_{stiff}$ ,  $\phi_1 = \phi_0$ ,  $\phi_2 = 0$ .
5. Use the DEM theory and the modelling method to calculate  $Vp_{Modeling} = f(K_0, \mu_0, \alpha_1, \alpha_2, \phi_1, \phi_2)$ .
6. If  $(Vp - Vp_{Modeling})^2 > \varepsilon$ , then  $\phi_1 = \phi_1 - \delta\phi$  and  $\phi_2 = \phi_2 + \delta\phi$ .
7. Repeat steps 4 and 5 until  $(Vp - Vp_{Modeling})^2 > \varepsilon$ , in such a way that  $\phi_{reference} = \phi_1$ ,  $\phi_{stiff} = \phi_2$ .
8. If the measured velocity  $Vp$  is lower than  $Vp_{reference}$ , use  $\alpha_1 = \alpha_{reference}$ ,  $\alpha_2 = \alpha_{crack}$ ,  $\phi_1 = \phi_0$ ,  $\phi_2 = 0$ .
9. Use the DEM theory and the modelling method to calculate  $Vp_{Modeling} = f(K_0, \mu_0, \alpha_1, \alpha_2, \phi_1, \phi_2)$ .
10. If  $(Vp - Vp_{Modeling})^2 > \varepsilon$ , then  $\phi_1 = \phi_1 - \delta\phi$  and  $\phi_2 = \phi_2 + \delta\phi$ .
11. Repeat steps 8 and 9 until  $(Vp - Vp_{Modeling})^2 > \varepsilon$ , so that  $\phi_{reference} = \phi_1$ ,  $\phi_{crack} = \phi_2$ .
12. The crack density  $\eta$  can be calculated as follows from both the crack-induced porosity and aspect ratio  $\eta = \frac{3\phi_{crack}}{4\pi\alpha_{crack}}$  (Hudson 1981).

## GEOPHYSICAL PORE TYPE PREDICTION FROM WELL LOG AND SEISMIC DATA

### Geophysical pore-type inversion from well log data

Log data from well A offshore Brazil are displayed in Fig. 7 as a function of depth. The lithology content, P-wave velocity, bulk porosity and water saturation will be used as the input of our pore-type inversion. Following the geophysical pore-type inversion scheme discussed in the previous section, the inverted stiff pores (red), reference pores (yellow) and cracks (blue) for the carbonate reservoir in well A are shown in Fig. 7(b). It is evident that there are variations in pore types from sample to sample. Reference pores make up a large percentage of the pore space in the carbonate section of well A. As shown in this figure, we observe a good agreement between the inversion result and those identified by the OMRI-CAST logs in the well (Fig. 7c). For example, the OMRI-CAST log depicts that fracturing takes place at a depth of 2696–2699 m and 2862–2865 m. Geophysical pore-type inversion in this depth interval tells us that pore space is primarily composed of cracks and interparticle pores and the predicted crack density can be as high as 0.1. At the depth interval of 2896–2899 m, inverted pore-type results indicate that the crack-like pores dominate the pore space, which is illustrated by the complex fracture network found in the OMRI-CAST log at the corresponding depth interval. The pore-type inversion result shows that there are some stiff

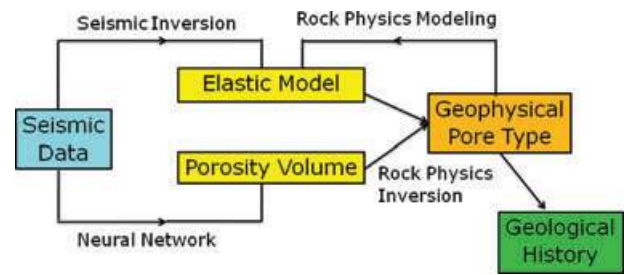
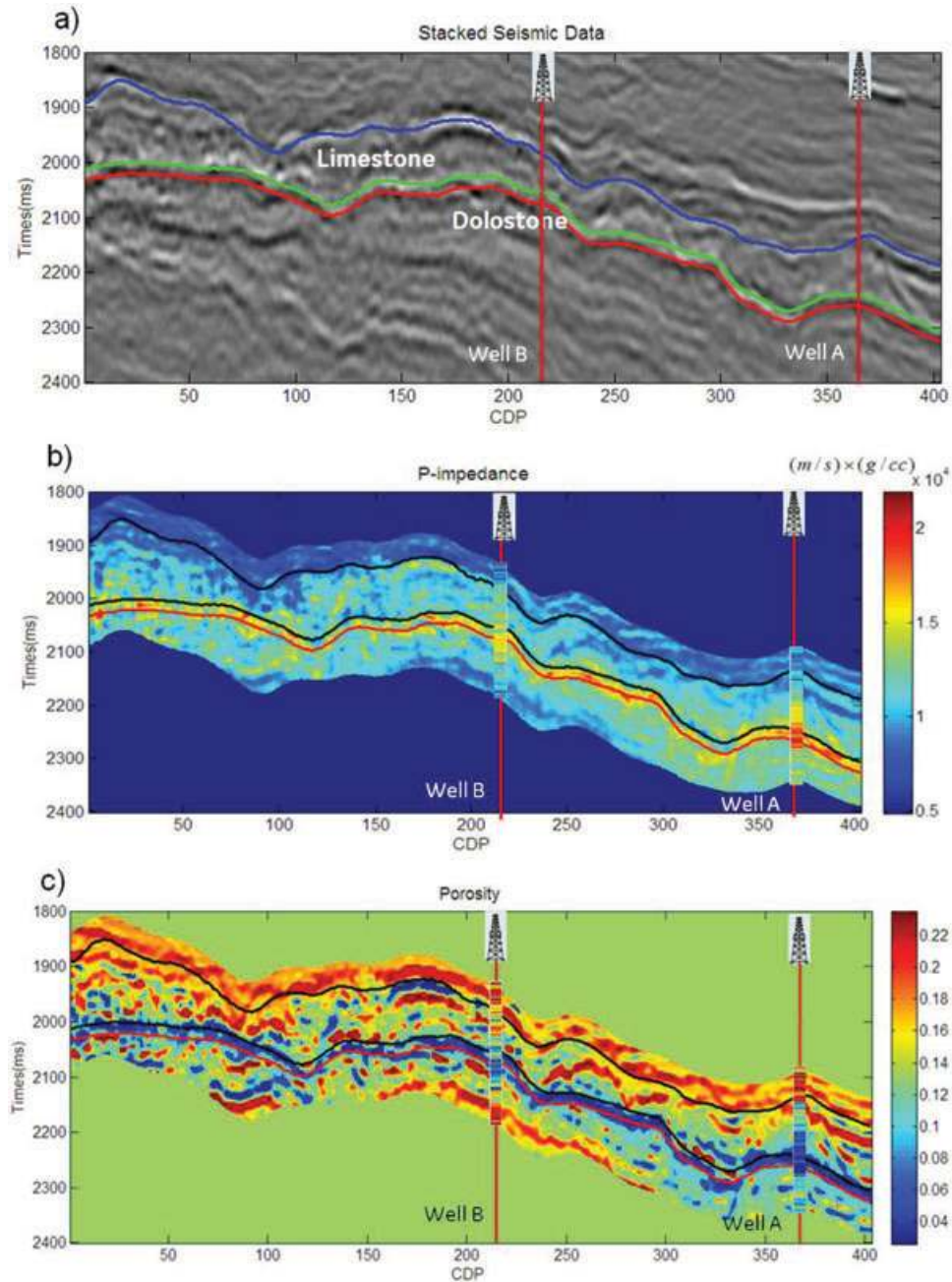


Figure 10 Schematic illustrations of a workflow used to predict geophysical pore-type distribution from seismic data. Elastic model and porosity volume are used as a bridge to link geophysical pore types to seismic data. Geological history can potentially be revealed based on the predicted geophysical pore-type distribution.

pores at the depth interval of 2884–2886 m and an irregular patch of vuggy porosity in the OMRI-CAST log is observed at the corresponding depth interval. The geophysical pore-type inversion result of well log B shown in Fig. 8 is also supported by the cracks and vuggy pores found in OMRI-CAST logs and core photos. This is especially the case in the interval between 2470–2500 m, where the predicted crack density is around 0.1. This is confirmed by the core photos that convey the information that rocks are intensely fractured in this interval. Moreover, some vugs, dissolved shell or molds can be seen from the OMRI-CAST log at the depth interval of 2523–2527 m, which is in agreement with the inversion result that the stiff pores and reference pores dominate the pore space.

Shear-wave velocity is not always available from log measurements, therefore people usually use the Greenberg-Castagna relationship to transform P-wave velocity to S-wave velocity. As we mentioned before, pore types in carbonates can complicate the  $Vp/Vs$  ratio. Consequently, based on the same rock physics modelling scheme to calculate P-wave velocity, we can use the inverted pore-type distribution to predict shear-wave velocity. Figure 9 displays the S-wave prediction based on our pore-type inversion result in the carbonate reservoir of well A. The predicted P-wave velocity is almost perfectly matching the original well log data. Moreover, both the predicted S-wave velocity based on the pore-type inversion result and the predicted S-wave velocity using the Greenberg-Castagna relationship work well in the upper carbonate reservoir. However, in the lower carbonate reservoir, the predicted S-wave velocity based on the pore-type inversion result shows a better agreement with the original S-wave velocity than the predicted S-wave velocity using the Greenberg-Castagna relationship. This is probably because the pore types in the



**Figure 11** (a) Section of the stacked seismic data, with the upper limestone unit and the lower dolostone unit marked in the targeted inversion area. (b) Section of inverted acoustic impedance from seismic. (c) Section of estimated porosity from seismic. The corresponding acoustic impedance and porosity log from wells A (CDP 211) and B (CDP 367) are plotted for comparison and show good agreement with the inversion results.

upper carbonate reservoir are dominated by both reference and stiff pores, which have little effect on the  $V_p/V_s$  ratio. However, the complex pore system occurring in the lower carbonate reservoir can result in strong S-wave velocity variations.

#### Geophysical pore-type prediction from seismic data

The workflow (Fig. 10) we propose to make an inference about the volume fractions of the different geophysical pore types from seismic data can be summarized as follows:

- 1) Elastic parameters (P- and S-impedances) can be inverted from prestack seismic data. Inverted elastic attributes at the well location should be calibrated with log measurements.
- 2) Porosity can be derived using geostatistical methods, or can be predicted from rock physical relationships and seismic data analysis. The estimated porosity volume at the well location should also be calibrated with porosity log data.
- 3) Perform the geophysical pore-type inversion using the extracted seismic property (elastic model and porosity volume) as input based on the developed inversion algorithm.
- 4) Use the predicted geophysical pore-type distribution and the related deposition environment to reveal the possible background geological history.

Stacked seismic data are shown in Fig. 11(a). The target inversion area is interpreted as a limestone unit in the upper reservoir and a dolostone unit in the lower reservoir. The reservoir rocks are considered to be clean with a relatively low clay volume. We first invert for acoustic impedance (Fig. 11b) from prestacked seismic data. Porosity (Fig. 11c) is predicted using neural network analysis on multiple attributes from seismic data (Hampson, Schuelke and Quirein 2001). Both the acoustic impedance and porosity are in good agreement with the log response. Figure 12(a) shows the shale content distribution from the target inversion interval of wells A and B, where the dominant shale content ranges from 0–0.10. Figure 12(b) displays the response of P-wave velocity to shale content's variation, which tells us that the P-wave velocity for reference pores has a 3–5% perturbation caused by shale content varying from 0–0.10. Shale content is assumed to be 5% for our lithology input, which represents average shale con-

tent in the target reservoir. In this case, we ignored the effects of fluid saturation due to the similarities of heavy oil's elastic properties to those of brine.

Figure 13(a,b,c) displays the geophysical pore-type inversion results from seismic data, which reveal that the reservoir rocks are intensively heterogeneous. The inverted reference porosity distribution indicates that interparticle pores dominate the pore space in this carbonate reservoir, whereas stiffer pores (vuggy and moldic) are sparsely present in the lower limestone unit. In addition, the predicted crack density suggests that both the upper limestone unit and the whole dolostone unit are possibly heavily cracked.

### Geological implications of geophysical pore-type distribution

Geological processes control the spatial distribution of pore type. On the other hand, the distributions of pore type contain clues to help decipher the geological history, thereby giving implications to reservoir characterization. Areas of high crack density in the upper limestone unit and the lower dolostone unit may represent permeability sweet spots for this carbonate reservoir, however they do not seem to show a good correlation with the faults distribution highlighted in Fig. 13(c). Since the upper limestone unit is porous, cracks in this unit are likely controlled by dissolution collapse. However, in the tight dolostone unit, fracturing could be more associated with differential compaction due to dolostone's brittleness. On the other hand, the stiff (vuggy and moldic) pores we observe in the lower limestone unit indicate that the dissolution might be more extensive in this unit. The impact of diagenetic

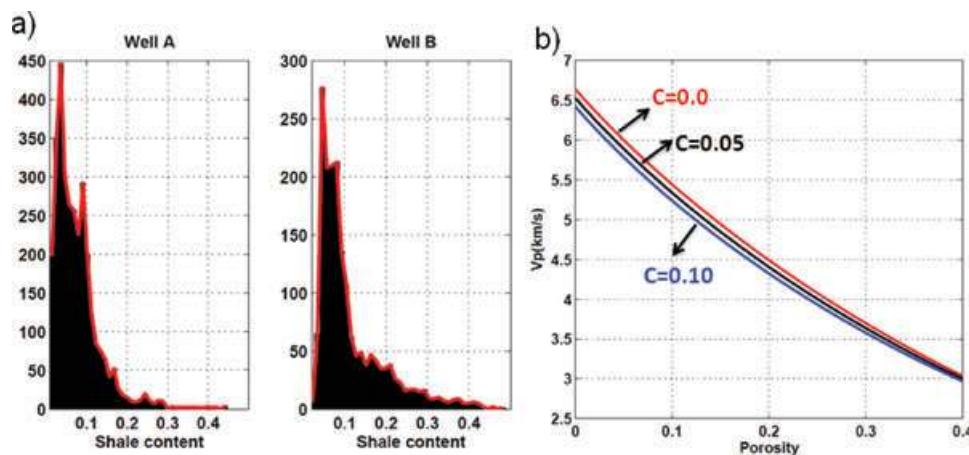
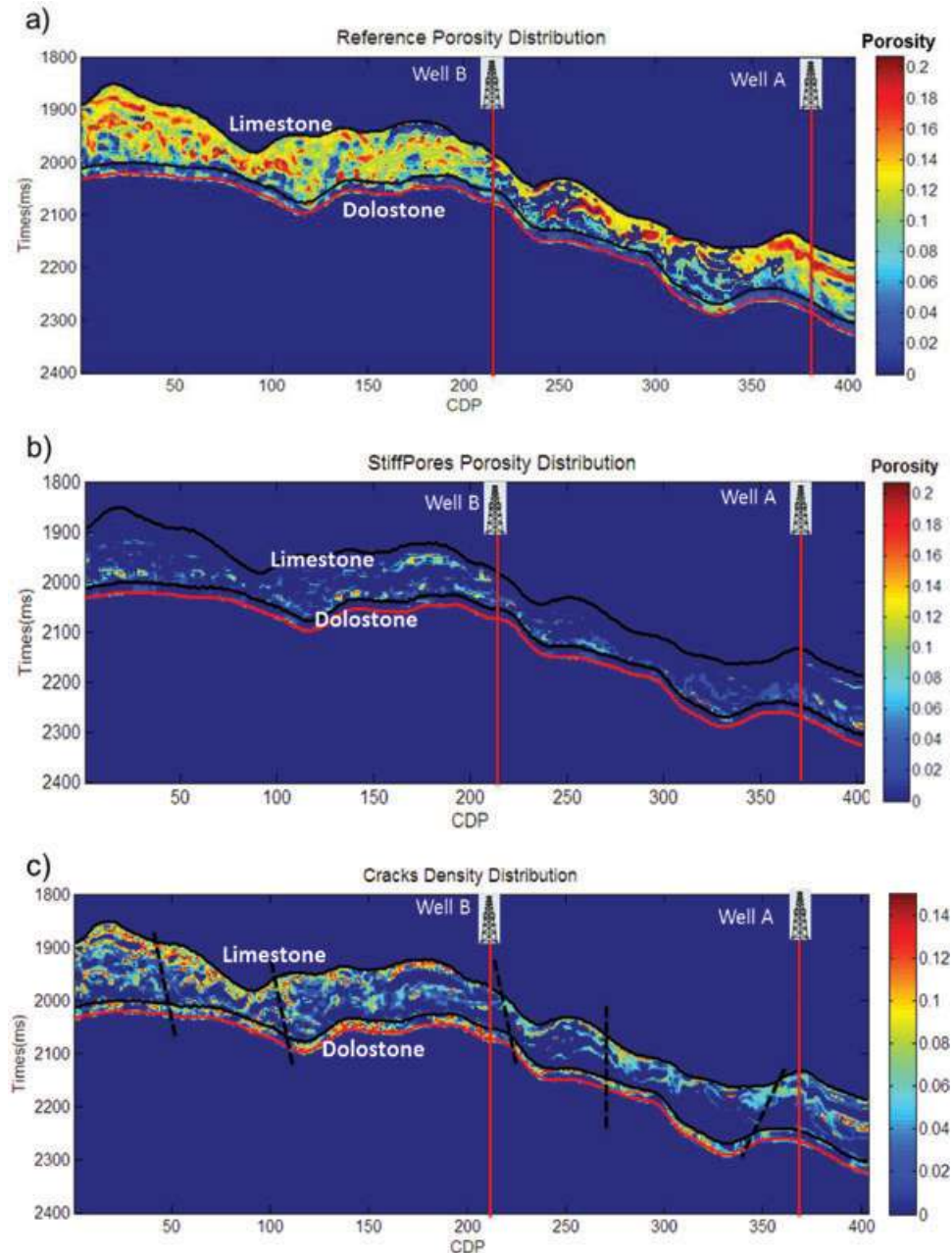


Figure 12 (a) Shale content distribution from wells A and B. (b) The response of P-wave velocity to the varying shale content for the reference pores. C indicates the shale content.





**Figure 13** Sections of geophysical pore-type distribution from seismic data at the target area: (a) reference porosity, (b) stiff pores porosity and (c) crack density. Faults identified from seismic interpretation are highlighted in (c). Well locations for well A at CDP 211 and well B at CDP 367 are also marked.

processes on the reservoir quality is sketched on the permeability-porosity cross-plot shown in Fig. 14. Normally, permeability is well correlated with interparticle or intercrystal porosity, while the presence of separate-vug porosity is, in contrast, mostly ineffective with regard to permeability. In addition to this, micro-fractures in carbonates can enhance per-

meability dramatically (Lucia 1995). In the upper limestone unit, after early consolidation, compaction and cementation, the pore space of the reservoir is reorganized by dissolution and fracturing. In the lower dolostone unit, dolomitization here is believed to play a valuable role in improving reservoir quality through increasing particle size in the mud-dominated

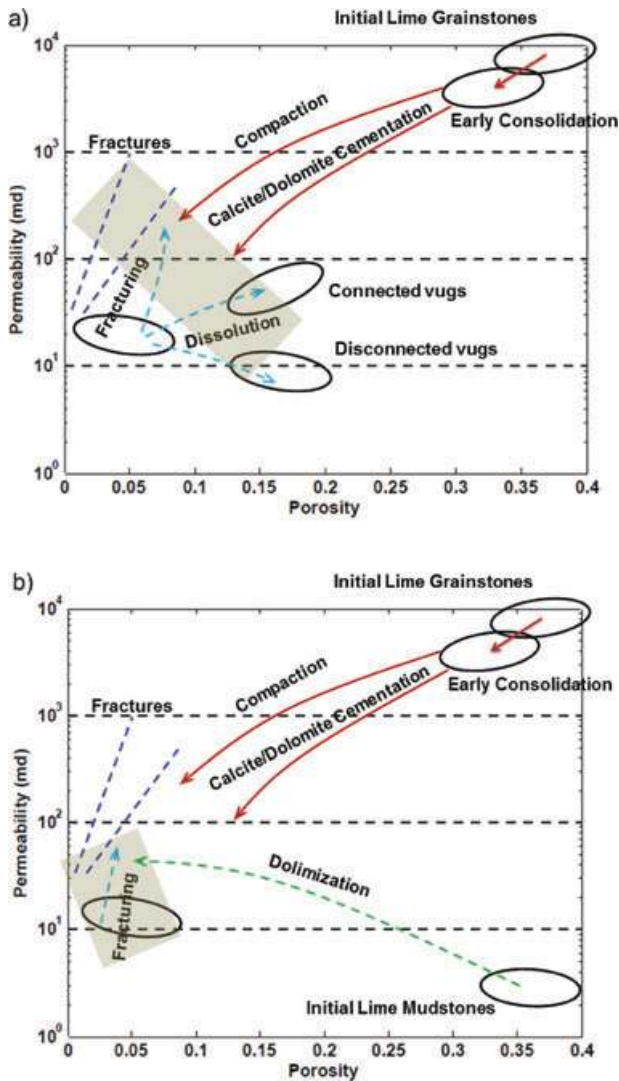


**Figure 14** Schematic illustrations of the diagenetic history's impact on reservoir quality for: (a) the upper limestone unit, (b) the lower dolostone unit. Circles indicate facies of carbonate, arrows represent geological processes that link different facies in the carbonate reservoir and shadow zones indicate the final product of diagenetic history.

fabrics by replacing the lime mud with medium-size dolomite crystals. Consequently, as the shadow zone indicates, this carbonate reservoir can be interpreted as the final product of dissolution, dolomitization and fracturing. Based on the porosity-permeability relationship, the upper limestone unit is identified as a potential sweet spot for reservoir development and production.

## DISCUSSION AND CONCLUSIONS

Pore geometries in carbonates control the fluid flow properties and are governed by geological history but the complexity of such pore structures defies a suitable prediction of pore-type distribution from geophysical measurements. In this paper, we demonstrated that three geophysical pore types (stiff pores, reference pores and cracks) can conveniently and effectively quantify effects of pore type on the elastic properties of carbonates. This study also shows that the proposed rock physics modelling and inversion scheme can yield a good quantitative characterization of pore type from well log data. Moreover, the S-wave prediction based on the pore-type inversion result also shows better agreement with original well log data than the Greensberg-Castagna relationship. To a larger degree, we expect that this rock physics scheme can potentially characterize porosity heterogeneity in carbonate reservoirs. It is demonstrated that core description, geological knowledge and well log and seismic data can be integrated to map the geophysical pore-type distribution in a carbonate reservoir offshore Brazil. Based on the predicted spatial pore-type distribution, we identified the likely diagenetic processes and interpreted how the product of fracturing, dissolution and dolomitization reorganize and redistribute pore space in a carbonate reservoir, thereby giving insight into reservoir description and reservoir model construction.

Several important points should be discussed regarding geophysical pore-type characterization in carbonate reservoirs. The inverted geophysical pore types are not sufficient to characterize the details of rock microstructures, they only represent the average elastic effective properties of a complex pore structure when a seismic wave propagates. On the other hand, fractures are generally a large-scale phenomenon that can be related to anisotropy and are often assessed by azimuthal seismic data. However in this work, we assume that cracks are randomly distributed and that the seismic wave is particularly sensitive to the presence of low-aspect ratio cracks. The schemes we proposed here are not able to fully characterize mesoscale fracture networks that are important for reservoir production. Besides, theoretically, when the compliant crack-like pores and stiff pores coexist in a pore system, cracks can be easily contracted and expanded under external wave excitation, hence squeezing the fluid into neighbouring stiff pores and generating squirt flow. Therefore, velocity dispersion can occur as the result of pore's elastic heterogeneity. The rock physics modelling approach we implemented in this study could not handle such dispersion effects that are associated with wave induced fluid flow. Ultrasonic well log data

and seismic measurements should be cautiously compared to understand the fluid substitution effects (Adam, Batzle and Brevik 2006). In our future work, we will consider applying poroelastic models to take into account wave induced fluid flow for fractured, porous carbonates. Finally, it is necessary to point out that there are always uncertainties associated with a geophysical pore-type inversion result as it depends on many factors: the quality of the seismic data, the number of wells, acoustic impedance used as input, porosity volumes, shale content and fluid content. All these factors should be carefully calibrated to allow more reliable predictions of geophysical pore-type distribution.

## ACKNOWLEDGEMENT

We thank Maersk oil and OGX for permission to publish the data.

## REFERENCES

- Adam L., Batzle M. and Brevik I. 2006. Gassmann's fluid substitution and shear modulus variability in carbonates at laboratory seismic and laboratory frequencies. *Geophysics* **71**, 173–183.
- Agersborg R., Johansen T.A., Jakobsen M., Sothcott J. and Best A. 2008. Effects of fluids and dual-pore systems on pressure-dependent velocities and attenuations in carbonates. *Geophysics* **73**, 287–323.
- Anselmetti F.S. and Eberli G.P. 1993. Controls on sonic velocity in carbonate rocks. *Pure and Applied Geophysics* **141**(2), 287–323.
- Anselmetti F.S. and Eberli G.P. 1997. Sonic velocity in carbonate sediments and rocks. In: *Carbonate Seismology* (eds I. Palaz and K.J. Marfurt), pp. 53–74. Geophysical Developments 6.
- Assefa S., McCann C. and Sothcott J. 2003. Velocities of Compressional and shear waves in limestones. *Geophysical Prospecting* **51**, 1–13.
- Baechle G.T., Colpaert A., Eberli G.P. and Weger R.J. 2007. Modeling velocity in carbonates using a dual porosity DEM model. 77th Annual International Meeting, SEG, Expanded Abstracts.
- Baechle G.T., Weger R. and Eberli G.P. 2005. Changes of shear moduli in carbonate rocks: Implication for Gassmann applicability. *The Leading Edge*, 507–510.
- Berryman J. 1992. Single-scattering approximations for coefficients in Biot's equations of poroelasticity. *Journal of Acoustic Society of America* **91**, 551–571.
- Brie A., Johnson D.L. and Nurmi R.D. 1985. Effect of spherical pores on sonic and resistivity measurements. 26th Annual Logging Symposium, SPWLA, 1 Paper W.
- Choquette P.W. and Pray L.C. 1970. Geologic nomenclature and classification of porosity in sedimentary carbonates. *AAPG Bulletin* **54**, 207–250.
- Dunham R.J. 1962. Classification of carbonate rocks according to depositional texture. In: *Classification of carbonate rocks* (ed. W.E. Ham), pp. 108–121. American Association of Petroleum Geologists Memoir.
- Eberli G.P., Baechle G.T., Anselmetti F.S. and Incze M.L. 2003. Factors controlling elastic properties in carbonate sediments and rocks. *The Leading Edge* **22**, 654–660.
- Hampson D., Schuelke J. and Quirein J. 2001. Use of multi attribute transforms to predict log properties from seismic data. *Geophysics* **66**, 220–236.
- Han D. 2004. Velocity of carbonate rocks. Annual Report, Rock Physics and Fluid Consortium.
- Hudson J.A. 1981. Wave speeds and attenuation of elastic waves in material containing cracks. *Geophysical Journal of the Royal Astronomical Society* **64**, 133–150.
- Jakobsen M. and Chapman M. 2009. Unified theory of global flow and squirt flow in cracked porous media. *Geophysics* **74**, 65–76.
- Jakobsen M., Hudson J.A. and Johansen T.A. 2003a. T-matrix approach to shale acoustics. *Geophysical Journal International* **154**, 533–558.
- Jakobsen M., Johansen T.A. and McCann C. 2003b. The acoustic signature of fluid flow in complex porous media. *Journal of Applied Geophysics* **54**, 219–246.
- Keys R.G. and Xu S. 2002. An approximation for the Xu-White velocity model. *Geophysics* **67**, 1406–1414.
- Kumar M. and Han D. 2005. Pore shape effect on elastic properties of carbonate rocks. 75th Annual International Meeting, SEG, Expanded Abstracts, 1477–1480.
- Kuster G.T. and Toksöz M.N. 1974. Velocity and attenuation of seismic waves in two-phase media, Part I: Theoretical formulations. *Geophysics* **39**, 587–606.
- Lucia F.J. 1995. Rock-fabric/petrophysical classification of carbonate pore space for reservoir characterization. *American Association of Petroleum Geologists Bulletin* **79**, 1275–1300.
- Lucia F.J. 1999. *Carbonate Reservoir Characterization*. New York, Springer-Verlag.
- Mavko G., Mukerji T. and Dvorkin J. 2009. *The Rock Physics Handbook: Tools for Seismic Analysis in Porous Media*. Cambridge University Press.
- Ogiesoba O.C., Wright W., Wang F., Popini M.V., Franco M.P., Lourenco A.T. and da Silva G.B.D. 2011. Seismic conditioning and attenuation of high-angle coherent noise in a mixed carbonate and siliciclastic setting, Campos Basin, offshore Brazil: A case study. *Geophysics* **76**(5), B199–B212.
- Rafavich F., Kendall C.H.St.C. and Todd T.P. 1984. The relationship between acoustic properties and the petrographic character of carbonate rocks. *Geophysics* **49**, 1622–1636.
- Ruiz F. 2009. *Porous grain model and equivalent elastic medium approach for predicting effective elastic properties of sedimentary rocks*. PhD thesis, Stanford University.
- Sain R., Chen G., Xu S. and Payne M.A. 2008. Carbonate rock physics: Geophysical and petrophysical pore types of carbonate rocks from an offshore carbonate field. 78th Annual Meeting, SEG, Expanded Abstracts, 1655–1699.
- Sayers C.M. 2008. The elastic properties of carbonates. *The Leading Edge* **27**, 1020–1024.



- Sun Y.F., Berteussen K., Vega S., Eberli G.P., Baechele G.T., Weger R.J. *et al.* 2006. Effects of pore structure on 4D seismic signals in carbonate reservoirs. 76th Annual International Meeting, SEG, Expanded Abstracts, 3260–3264.
- Vanorio T., Scotellaro C. and Mavko G. 2008. The effect of chemical and physical processes on acoustic properties of carbonate rocks. *The Leading Edge* 27, 1040–1048.
- Wang Z., Hirsche K.W. and Sedgwick G. 1991. Seismic velocities in carbonate rocks. *Journal of Canadian Petroleum Technology* 30, 112–122.
- Wu T.T. 1966. The effect of inclusion shape on the elastic moduli of a two-phase Material. *International Journal of Solids and Structures* 2, 1–8.
- Xu S. and Payne M.A. 2009. Modeling elastic properties in carbonate rocks. *The Leading Edge* 28, 66–74.